Numerical simulation of regenerative chambers for glass production plants with a non-equilibrium heat transfer model

CARLO CRAVERO
Dipartimento di Ingegneria Meccanica, Energetica, Gestionale e dei Trasporti (DIME)
Università di Genova
Via Montallegro 1 – 16145 Genova
ITALY
cravero@unige.it

DAVIDE MARSANO
Dipartimento di Ingegneria Meccanica, Energetica, Gestionale e dei Trasporti (DIME)
Università di Genova
Via Montallegro 1 – 16145 Genova
ITALY
davide.marsano@edu.unige.it

Abstract: - Regenerative heat exchangers used in glass industry are complex system owing to the transient nature of their cycle, as well as to the complexity of the heat exchange phenomena involved: mixed convection during the cold period (air flux) and combined presence of radiation ad forced convection during the hot period (exhaust gases flux). The present work describes a method to simulate the behaviour of such regenerators. The fluid domain is solved as a porous domain with friction and heat transfer effects modelled as source term in the momentum and energy equations respectively. In this work a so called "non-equilibrium thermal model" is developed as an improvement with respect to a previous model based on a volumetric heat transfer in the porous domain calibrated from experimental data. The improved approach models the heat transfer process through the heat transfer coefficient that is more fundamental and does not require experimental data.

Key-Words: - Glass production plant, energy efficient regenerators, CFD

1 Introduction

The specific consumption of a generic glass furnace is about 4000 kJ/kg glass received from fuel. About 1500 kJ each kg of glass is recovered in combustion air using regenerators [1]. An increase in the preheat temperature of combustion air leads to a decrease of the specific consumption and a higher temperature inside the furnace. The regenerative chamber for a glass furnace allows the saving of a considerable amount of energy, which would otherwise be lost. In Italy during 2004 the glass industry absorbed 1.33 Mtoe (4% of total industrial consumption). A regenerative chamber (Fig.1) is composed of a series of refractory bricks, located in the central part, that are responsible to store heat when hot gases from combustion flow ("hot phase") and to return it to the combustion air in the so-called "cold phase". In fact the process is cyclic: the exhaust gas from combustion enter from the top chamber at approximately 1400 C and exit the regenerative chamber at about 800 C; after about 20 minutes the air is fed from the bottom of the chamber to reach a temperature of about 1100 C at the top.

The efficiency of this process is 60-68 % against a theoretical limit value of 75-78% and this model of regenerator, conceived in 1850 by Martin-Siemens, is still the best practical solution. However, the growing concern about power consumption and pollutant emissions, requires a more strategic and efficient use of these technologies. In this prospect, a CFD approach could bring a valuable input to the design process, providing detailed analysis of consolidated solutions and support for the design of innovative concepts.

The present work is a contribution to this field and the obtained simulation approach is in current industrial use for regenerative chambers design. The problem of numerical modelling for regenerative heat-transfer components has been tackled by several authors for different applications [2,3,4] and the main

problem is the effective modelling of the complex internal structure for CFD detailed analysis. The performance prediction of regenerative chambers is strategic to estimate the overall performance of glass furnaces. Sardeshpande [7] presents a regenerator blockage prediction model and the effect of leakage on the performance of fixed matrix regenerator was studied by Skiepko and Shah [8]; regenerator performance evaluation using numerical techniques was discussed by Foumeny and Pahlevanzadeh [9].

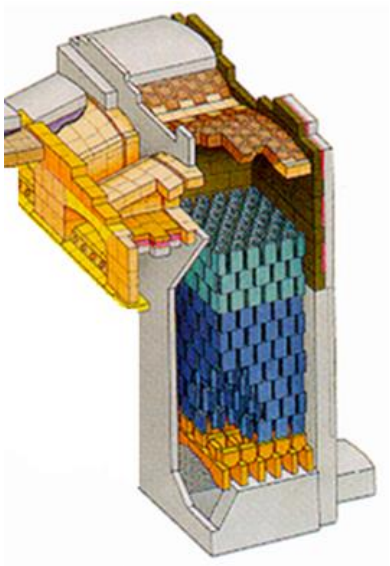

Figure 1. Regenerative chamber of a glass furnace view with internal bricks.

The basic idea of the present approach is to replace the real geometry of the bricks, in the checkers zone, with a porous domain. The discretization of the real geometry of the bricks would require a too expensive mesh with an impractical CFD process to use routinely in the industrial design chain. The model must ensure a physical equivalence with the real component on these three main effects on the flow: the total pressure losses, the transfer of thermal energy (from the bricks to air and from waste gas to the bricks) and buoyancy forces (due to solid-fluid temperature gradients and chamber height). The authors have developed a first CFD model for this type of regenerative chambers [5, 6] with a simplified approach for the heat flux into the porous domain; the overall heat flux inside the chamber was obtained by known (estimated or from plant operation data) inlet and outlet temperature distributed linearly inside the domain. In order to be able to take into account the effect of the bricks layout and of the cruciform geometry on the heat transfer process inside the chamber, the previous model has been improved with the present version that predicts the heat transfer inside the chamber from a given distribution of the heat transfer coefficient inside the porous domain. This model is called "non-equilibrium" model and it is an effective improvement for the regenerator simulation because it allows the effect of cruciform layout and geometry to be assessed during the design phase when the strategic decisions for the component layout are taken. The heat transfer coefficient prediction is the critical aspect for the model: it has been developed using valuable data from literature [10, 11] and with the approach described in the following paragraphs.

2 CFD Approach

The Ansys CFD commercial suite has been used with the ICEM-CFD code for CAD repairing and meshing and the Fluent flow solver. The RANS set of equations is solved with the SST turbulence closure. In Fig.2 the computational domain is shown with the central domain (where the checkers are stored) modelled as a porous domain. As described in [5, 6] source terms in the momentum and energy equations are added to take into account friction and heat flux effects into the porous domain. The source term in the momentum equation is composed of two parts: viscous losses and inertial losses. The arrangement of the refractory bricks in the checkers zone is such as to form a kind of tube bundle with variable section, depending on the shape of the brick, with typical hydraulic diameter that varies between 150 to 200 mm. This suggests an anisotropic formulation for the porous source, equations (1-2-3):

$$S_{M,x} = -\frac{\mu}{K^T_{perm}} - K^T_{loss}\frac{\rho}{2}|v|v_x \qquad (1)$$

$$S_{M,y} = -\frac{\mu}{K^S_{perm}} - K^S_{loss}\frac{\rho}{2}|v|v_y \qquad (2)$$

$$S_{M,z} = -\frac{\mu}{K^T_{perm}} - K^T_{loss}\frac{\rho}{2}|v|v_z \qquad (3)$$

In facts, it identifies a preferential direction of the flow in the porous domain, in this case along the vertical direction; the flow along the other directions is inhibited with the corresponding porous coefficients K^T_{perm} e K^T_{loss} obtained by multiplying by 10^2 the coefficients for the preferred direction K^S_{perm} e K^S_{loss}. These coefficients are obtained from a simulation campaign over a single module of bricks

with its real 3D geometry by varying the mass flow rate and thermal conditions as detailed in [5, 6]. The fundamental thermal effects inside the regenerative chamber, in addition to the porous resistance, due to heat transfer between the bricks and the fluid, need to be modelled inside the porous domain. In previous work [5, 6] the equilibrium thermal model has been developed and applied to the simulation of industrial regenerative chambers. The heat source was obtained from an estimate of the fluid temperature distribution inside the porous domain, integrated to get the heat flux released by the exhaust gases or absorbed by the air:

$$S_{M,therm} = m' \int_{T_{bot}}^{T_{top}} c_p dT \qquad (4)$$

The need for the temperature distribution is evident; it can be estimated as a linear variation inside the chamber from bottom to top sections where the temperature values (T_{bot} e T_{top}) are either known from the plant operating condition or from design values. To overcome the need for external data the non-equilibrium thermal model has been set up. The heat flux is obtained from the heat transfer coefficient between fluid and solid phases and its distribution inside the chamber. The above heat transfer coefficient is different for cold and hot cycles, depends on the brick geometry and it is estimated from a simulation campaign (as for the resistance coefficients) performed on a brick module with its actual CAD 3D geometry.

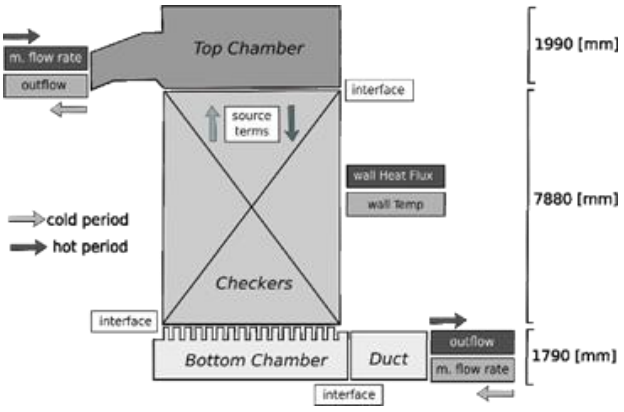

Figure 2. Schematic view of the regenerator CFD model with relevant boundary conditions

The heat transfer process for cold and hot cycle is different; in the cold cycle the air flows from the bottom section to the top section into the hot regenerative chamber with strong buoyancy effects and an overall natural convection process. On the contrary, in the hot cycle, the exhaust gases flow into the chamber from the top to the bottom section with a negative pressure gradient (higher pressure for the exhaust gases in the top section from the combustion process); the forced convection heat transfer model is therefore more appropriate. Two different CFD models are needed for the above thermal processes. In the following sections the set up and validation of the above models for the hot (forced convection) and cold (natural convection) cycles are described.

2.1 Forced convection CFD model

The experimental work from [12] has been used as reference case for the setup of the CFD model for the hot phase where the forced convection effect is dominant. In the reference work, the convective heat transfer coefficient inside a channel of rectangular section was measured with the circuit sketched in Fig.3 and using a deposition of liquid crystals on the heated bottom wall of the channel.

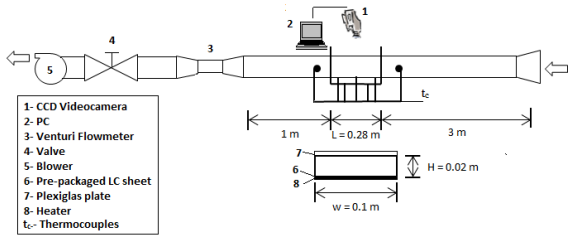

Figure 3. Schematic layout of the experimental setup and test section for the forced convection validation [12]

The configuration of the experimental setup is sketched in Fig. 3 and the complete data are given in [12]. The channel has been modelled in 3D with two different structured meshes with different mesh clustering at the wall to obtain a Y+ of about 30 (60x15 nodes) or close to one (80x40 nodes) in order to compare the results from the use of wall-functions or low-Reynolds terms in the numerical treatment of the k-ω SST turbulence model. The following boundary conditions are set: uniform heat flux of 1000 W/m^2 at the hot wall and a fully developed turbulent flow profile at inlet with Re=90.000. Air ideal gas with polynomial variation of thermodynamic properties is used.

The standard 2ND order SIMPLE numerical scheme has been activated. In Fig.4 the finest mesh is reported for a section of the channel in the streamwise direction.

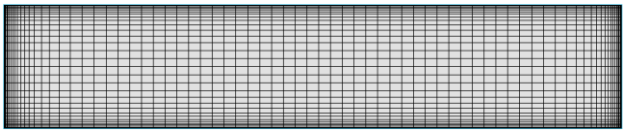

Figure 4. Mesh section of the 3D test section along the flow direction

In Fig.5 the contours of temperature at the hot wall obtained with the coarser mesh with wall-function treatment (up) and the contours for the mesh with Y+ close to one (down) are shown. Minor differences are observed mainly at the inlet section due to the different development of the boundary layer with the two grids. With the temperature values located along the main axis of the hot wall (T_{LC}) the local convective heat transfer coefficient is calculated:

$$h = \frac{q_{conv}}{T_{LC} - T_{air,z}} \tag{5}$$

where:

$$T_{air,z} = T_{air,0} + \frac{(q_{conv} A_{hot})(z/L)}{m' c_p} \tag{6}$$

then the Nusselt number ratio to the Dittus-Boelter's Nusselt number (valid for smooth circular tubes with fully developed turbulent flow) can be introduced:

$$\frac{Nu}{Nu_0} = \frac{hD/k}{Nu_0} \tag{7}$$

where

$$Nu_0 = 0.023 \mathrm{Re}^{0.8} \mathrm{Pr}^{0.4} \tag{8}$$

The above relations have been used to compare the Nusselt number ratio along the hot surface longitudinal centreline between the experimental data and the numerical solutions. Fig.6 shows comparison with the experimental data and the values from both CFD simulations with the different meshes. The diagram shows a correct trend of both simulations with an average error of 8% with coarser grid (wall-functions) and 6% with finer mesh. It can be observed that the simulation with Y+=1 underestimates the experimental data, while with wall functions the heat transfer is overestimated.

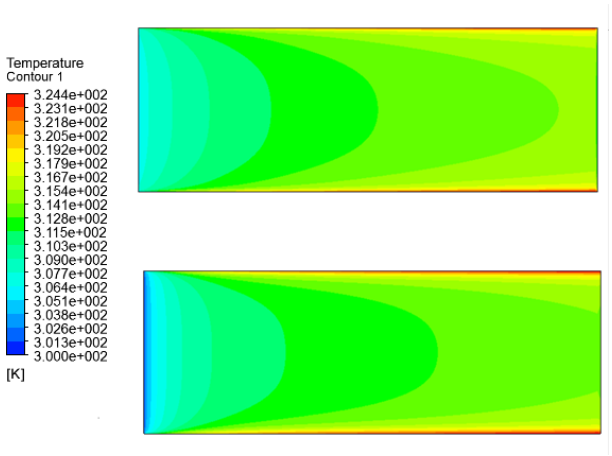

Figure 5. Surface temperature distributions in the hot wall, for the cases with wall functions (up) and with wall treatment (down)

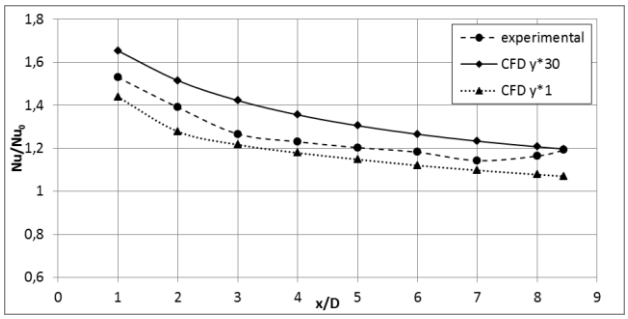

Figure 6. Nusselt number ratio along the test section: comparison between numerical results and experimental data

Nevertheless, both results are considered acceptable for the scope of the model and the use of wall-function is selected as the option for the regenerator non-equilibrium model because it allows the use of coarser meshes without significant loss of accuracy.

2.2 Natural convection model

The experimental data from [13] have been selected as reference case for the CFD model in the cold phase when the natural convection physical mechanism is the most appropriate. The temperature distribution inside a vertical channel of rectangular section, obtained between two adjacent walls, has been measured with a set of thermocouples and the Nusselt number along the hot wall is available. In Fig.7 a schematic view of the experimental setup is reported and all the data are available from [13].

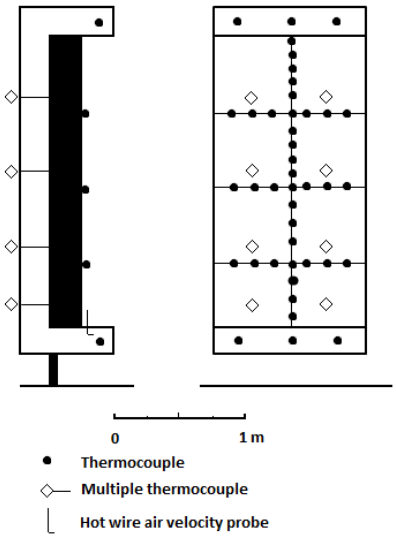

Figure 7. Scheme of the experimental model for free convection [13]

A single block structured mesh with 500.000 elements with wall density for a Y+ of about 30 has been generated. The numerical simulations have been set as steady incompressible flow with the k-ω SST turbulence model and the 2ND order SIMPLE numerical scheme. In this application, the buoyancy effect is activated to model the density gradient from temperature values in the Boussinesq approach. The boundary conditions are imposed as followed: uniform heat flux of 48 W/m^2 at the hot wall, flow velocity of 0,27 m/s (301,6 K temperature) at the inlet.

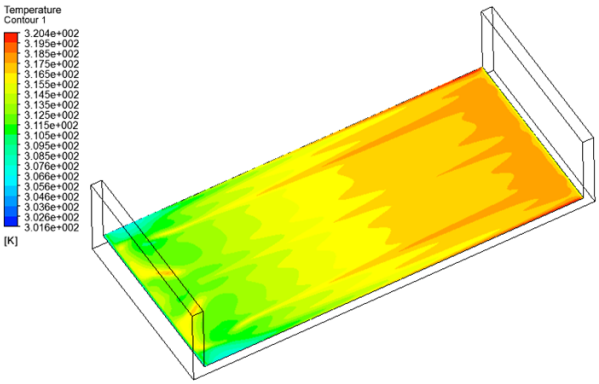

Figure 8. Surface temperature distributions at the hot wall

Fig.8 shows the temperature contours at the hot wall from the numerical simulation. In Fig.9 the experimental local temperature values along the height of the channel are compared to the numerical results.

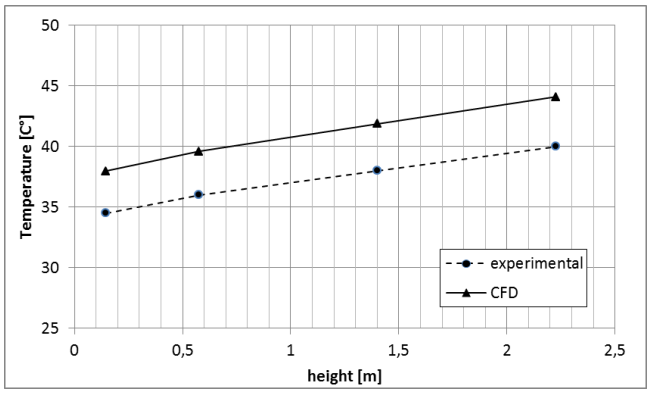

Figure 9. Temperature profiles along the channel in natural convection model

The correct trend is captured by the CFD analysis and a maximum error of 10% (in the hot wall) is detected. The CFD model with the above setup is considered adequate for the simulations of the checkers in the regenerative chamber during the cold phase.

2.3 Prediction of flow resistance coefficients

The source terms in the porous model associated to the flow resistance, eq.1-2-3, are obtained with a simulation campaign on a model based on one channel made of two smooth refractory checkers with their real geometry. The flow domain in the channel is discretised with an unstructured mesh and the boundary conditions are set according to [4] where useful experimental data are presented on a similar application. At the inlet boundary temperature and flow rate (air during cold phase or gases for the hot phase) are fixed. According to the above experimental data at the wall boundaries a thermal flux distribution is given (Fig.10) for the cold phase simulation. When the hot phase is simulated, the wall temperature distribution is the one obtained from the cold phase analysis. The waste gas in the hot phase are modelled as a multi-species fluid, with the following composition: 2.3% oxygen, 11.9% carbon dioxide, 17.1% water and 68.7% nitrogen. Moreover, due to presence of CO2 the radiation P1 model is also considered. The pressure drops coefficients for the regenerator, for both cold and hot phases, are obtained by changing the inlet flow rate (inlet flow velocity) in a suitable operating range; the resistance porous coefficients, required by the porous domain model (eq.1-2-3), are determined using a parabolic regression. In the present application a five meters long channel module has been considered and discretized with an unstructured mesh of about 600 kCells. An inlet air temperature of 420 [K] is fixed in

the cold phase and 1410 [K] for the gases in the hot phase.

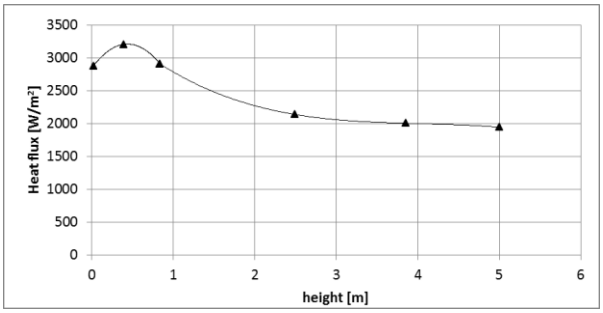

Figure 10. Profile of the regenerated heat flux for the cold period

In Fig.11-12 the pressure drops obtained by changing the inlet flow rate (inlet flow velocity) are shown for the cold and hot phase respectively.

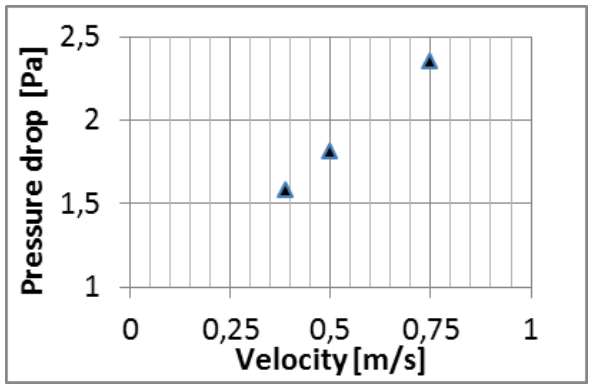

Figure 11. pressure drops for the cold phases

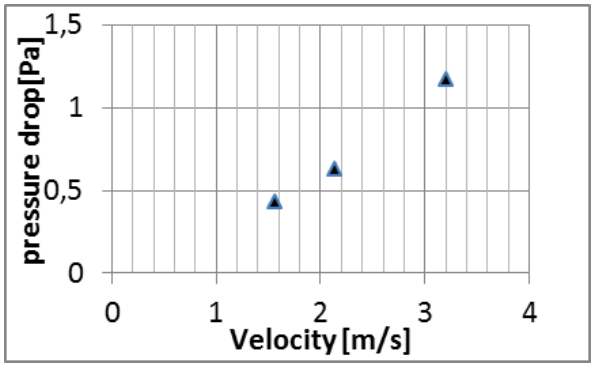

Figure 12. pressure drops for the hot phases

From the above values, the Inertial Resistance Factor (K^S_{perm}) and the Viscous Inertial Resistance Factor (K^S_{loss}) needed by eq.1-2-3 are obtained with the following relations:

$$\Delta p = cv^2 + dv + e \tag{9}$$

$$K^S_{perm} = \frac{2c}{\rho L} \tag{10}$$

$$K^S_{loss} = \frac{d}{\mu L} \tag{11}$$

2.4 Prediction of heat transfer coefficients

A conjugate heat transfer analysis is performed in the channel model in order effectively simulate the heat transfer process in the cold and hot phases taking into account the thermal inertia of the solid phase; the 3D channel model is therefore completed with the solid phase (bricks geometry) that is meshed accordingly as reported in Fig.13.

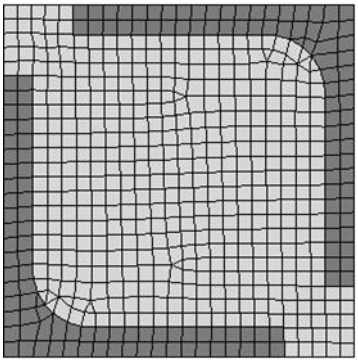

Figure 13. mesh section of the 3D channel model with solid phase meshed (dark grey)

Unsteady analysis are performed to reproduce the cold-hot phase change that has a typical frequency of 20 minutes. The simulation process starts with a first guessed linear temperature distribution inside the channel solid phase; the simulations are repeated by imposing the solid phase temperature from the previous analysis until convergence. When the first converged process is obtained, the cold phase (inlet air) is simulated using the solid temperature distribution from the hot phase analysis and vice versa for the hot phase (inlet gases). Fig. 14-15 show the distributions of the heat transfer coefficients for the air and waste gas cases obtained in the present sample application and used in the non-equilibrium thermal model of the regenerator. The heat transfer coefficient is calculated in the same way with eq.5, where in this case the subtrahend in the denominator Tfluid,z is the temperature in the centerline of the channel calculated with the CFD simulation.

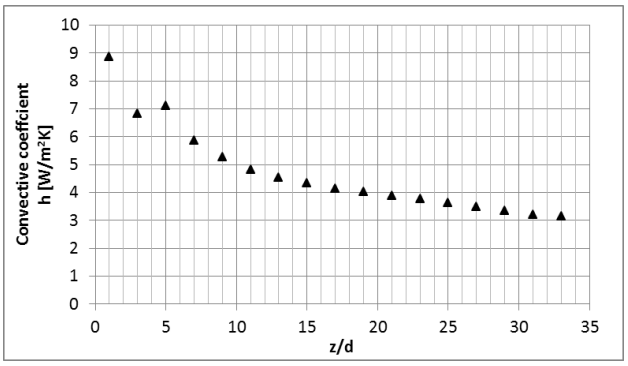

Figure 14. Convective heat transfer coefficient for air along the channel

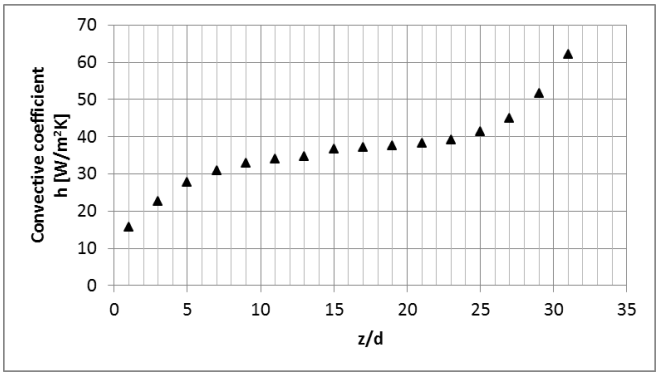

Figure 15. Convective heat transfer coefficient for waste gas along the channel

With the above distributions all the data required by both thermal models for the regenerative chamber analysis are complete and the simulation of the regenerator, at a given operating point, can be performed.

3 Application of thermal models to a regenerative chamber

The geometry of a regenerative chamber installed in an existing glass furnace plant has been modelled and simulated with both thermal models. The geometry of the chamber in the lower part is made of several arches for structural reasons (Fig.2) and this complicates the mesh generation process with structured grids, especially for the non-equilibrium thermal model where a conformal mesh at both ends of the porous domain (central volume domain) is required by Fluent CFD code. The ICEM-CFD code has been used for the mesh generation process and a multiblock structured mesh for the bottom chamber and the checkers zone using the blocking approach has been created; the top chamber domain (Fig.2) is meshed with an unstructured grid due to the difficult match between the bottom chamber and the geometry at the top. The mesh conformity at both ends of the porous domain is obtained by extruding the surface mesh in the vertical direction. In Fig.16, the view of a mesh section is shown.

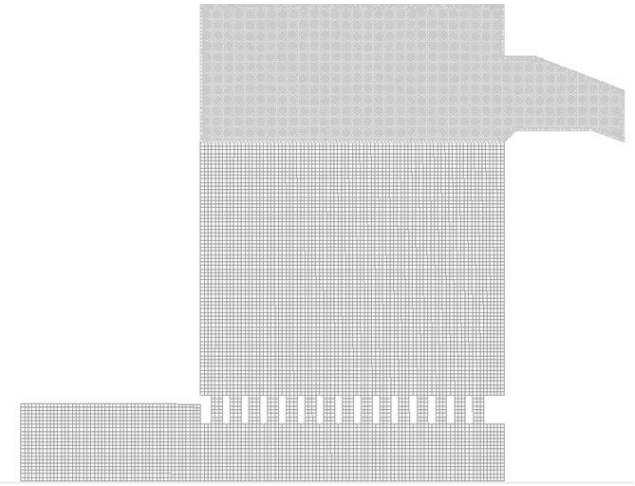

Figure 16. Mesh section for regenerative chamber (in dark grey the top chamber meshed with an unstructured grid)

The resistance coefficients for the porous domain have been obtained from the pressure drops in Fig.11-12 and the k-ω SST turbulence closure has been selected. Air inlet temperature of 420 [K] and velocity of 0.75 [m/s] have been fixed as boundary conditions for the cold phase and a linear distribution of the heat transfer coefficient from 8.9 [W/m^{2}K] to [3.2 W/m^{2}K] (that approximate the distribution from Fig.14) in case of non-equilibrium thermal model has been given into the porous domain. In case of equilibrium thermal model the heat source of 26.8 [W/m^3] into the porous domain is obtained by integrating a temperature distribution between 425 [K] and 1100 [K]. The numerical simulations have been set with a SIMPLE numerical scheme of 2ND order and considered fully converged after 500 iterations.

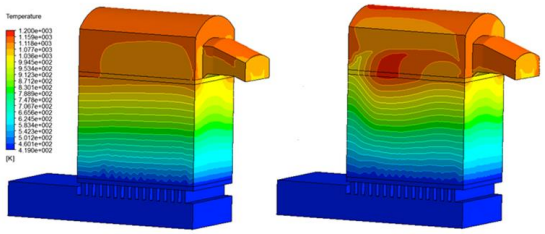

Figure 17. Cold phase surface temperature distributions for non-equilibrium (left) and equilibrium (right) thermal models

In Fig.17 the surface temperature distributions for non-equilibrium (left) and equilibrium (right) thermal models are reported. Fig. 18-19 show the average temperature and relative pressure distributions from bottom to top inside the porous domain for both models respectively. A remarkably good agreement is shown.

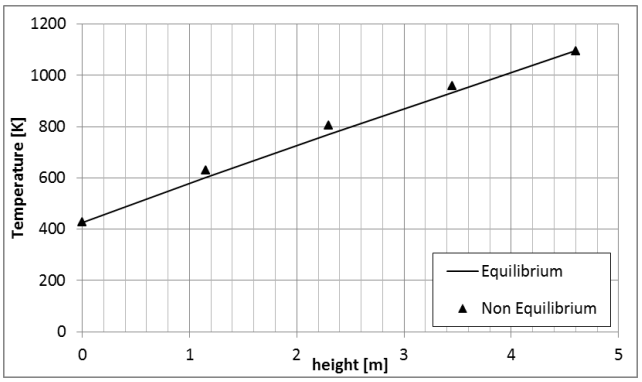

Figure 18. Average temperature distributions inside the porous domain

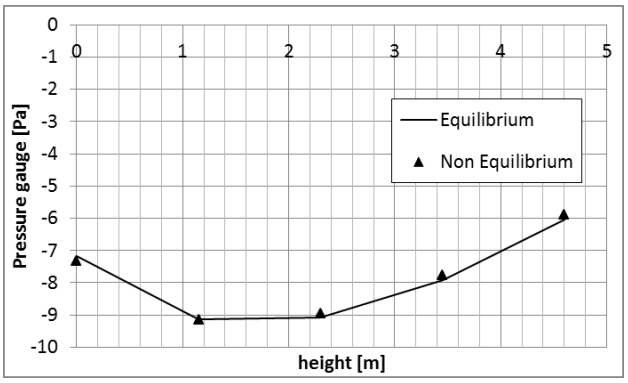

Figure 19. Average relative pressure distributions inside the porous domain

In the hot phase simulation the gas inlet temperature and the flow rate have been fixed equal to 1408 [K] and 2.72 [m/s] respectively. For the equilibrium thermal model the heat source is obtained by integrated a temperature distribution inside the porous domain with values of 1408 [K] and 825 [K] at top and bottom respectively. The heat transfer coefficient distribution of Fig.15 has been used inside the porous domain for the non-equilibrium thermal model.

In Fig.20 the surface temperature distributions for non-equilibrium (left) and equilibrium (right) thermal models are reported. It can be noticed that the temperature distribution in the Non-Equilibrium thermal model has a more linear trend with respect to the simpler equilibrium model that shows some inaccuracy in the thermal distributions (surface contours) due to the lack of constraints in the heat transfer process inside the chamber.

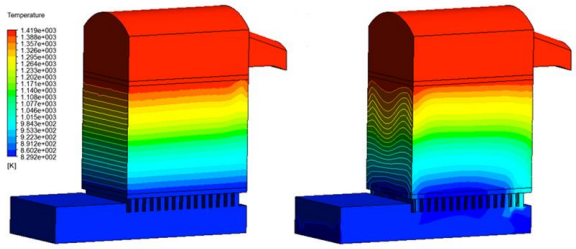

Figure 20. Hot phase surface temperature distributions for non-equilibrium (left) and equilibrium (right) thermal models

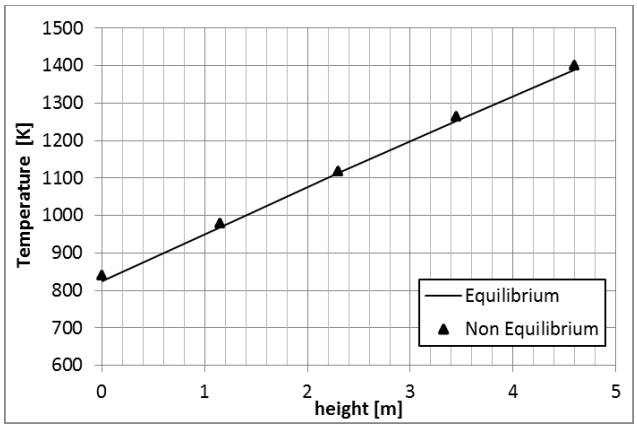

Figure 21. Average temperature distributions inside the porous domain

Fig. 21-22 show the average temperature and relative pressure distributions from bottom to top inside the porous domain for both models respectively. A very good agreement between the two models is observed.

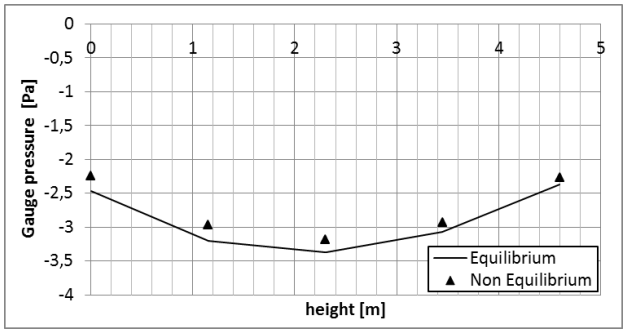

Figure 22. Average relative pressure distributions inside the porous domain

4 Conclusions

The proposed non-equilibrium thermal model for regenerator performance prediction has been applied

to the simulation of an existing configuration. The agreement and coherence with the results of the previous equilibrium model have been confirmed. The present model has a greater potential for design purposes of new configurations because it does not rely upon experimental (or operational) data for the heat flux modelling inside the chamber but is based upon more fundamental physical data like heat transfer coefficients; these are obtained with the proposed CFD procedure starting from the real geometry of the checkers that form the core of the regenerator and that drive their performance.

Aknowledgments:

This model and the CFD applications to glass industry presented have been developed within the PRIMEGLASS European Project (LIFE12 ENV/IT/001020) framework coordinated by Stara Glass Srl (Genova) in partnership with Università di Genova (Genova) and Stazione Sperimentale del Vetro (Venezia). Sara Glass Srl has kindly provided all the experimental and operational data used in the present application.

References:

[1] Tata Energy Research Institute. Practical energy audit manual: glass industry, prepared for Indo-German energy efficiency project, August; 1999.

[2] Koshelnik, A.V, *Modelling operation of system of recuperative heat exchangers for aero engine with combined use of porosity model and thermo-mechanical model.* Glass and Ceramics 2008. 65, 9-10, 301-304

[3] Zarrinehkafsh, M.T.; Sadrameli, S.M, *Simulation of fixed bed regenerative heat exchangers for flue gas heat recovery*. App Therm Eng 2004 24, 373-382

[4] Y. Reboussin, J.F. Fourmigué, JF Marthy Ph, Citti O., *A numerical approach for the study of glass furnace regenerators,* App Therm Eng 2005, 25, 2299-2320.

[5] Basso D, Briasco G, Carretta M., Cravero C, Mola A., *CFD simulation of regenerative chambers in glass industry to support the design process for thermal efficiency improvement,* Int. CAE Conference, Pacengo del Garda (Italy), 27-28 October 2014

[6] Basso D, Cravero C, Reverberi A.P *CFD analysys of regenerative chambers for energy efficiency improvement in glass production plants,* Fabiano B. Energies 2015, 8, 8945-8961

[7] Sardeshpande V, Anthony R, Gaitonde U.N, Banerjee R. *Performance analysis for glass furnace regenerator,* App Therm Eng 2011, 88, 4451-4458

[8] Skiepko T, Shah RK. *Modeling and effect of leakages on heat transfer performance of fixed matrix regenerators.* Int J Heat Mass Transfer 2005, 48, 1608-32

[9] Foumeny EA, Pahlevanzadeh. *Performance evaluation of thermal regenerators.* Heat Recov Syst CHP 1994; 14 (1):79-84

[10] Yazicizade AY *Untersuchung der Warmeubertragung und Druckabfalls in regenerator.* Glastechn Ber 1996, 39, 203-17

[11] Zanoli A, Leahy WD, Vidil R, Lagarenne D. *Experimental studies of thermal performance of various cruciform regenerator packing.* Glass Technol 1991;32(5):157-62

[12] Tanda G, Abram R, *Forced Convection Heat Transfer in Channels with Rib Turbulators Inclined at 45 deg,* Journal of Turbomachinery, April 2009, 131, 021012: 1-10

[13] La Pica A, Rodonò G, Volpes R. *An experimental investigation on natural convection of air in a vertical channel,* Int J Heat Mass Transfer 1993, 36, 611-616